B Physics at SLD

S. Willocq[a]

[a]Stanford Linear Accelerator Center
Stanford University, Stanford, CA 94309, USA

Representing the SLD Collaboration*
Stanford Linear Accelerator Center
Stanford University, Stanford, CA 94309, USA

We review recent B physics results obtained in polarized e^+e^- interactions at the SLC by the SLD experiment. The excellent 3-D vertexing capabilities of SLD are exploited to extract precise B^+ and B_d^0 lifetimes, as well as measurements of the time evolution of $B_d^0 - \overline{B_d^0}$ mixing.

*Presented at the 5th Topical Seminar on The Irresistible Rise of the Standard Model, 21-25 April 1997,
San Miniato al Todesco, Italy.*

1. INTRODUCTION

The results presented here are based on samples of approximately 50,000 and 100,000 $e^+e^- \rightarrow Z^0 \rightarrow$ hadrons events with longitudinally polarized electrons collected by the SLD experiment during the 1993 and 1994–95 data taking periods, respectively. During these periods, the average measured polarization was $(63.0 \pm 1.1)\%$ and $(77.2 \pm 0.5)\%$. A description of the detector can be found in Ref. [1]. B^+ and B_d^0 lifetime results are presented in Sec. 2 and B_d^0–$\overline{B_d^0}$ mixing measurements are discussed in Sec. 3.

2. B^+ AND B_d^0 LIFETIMES

Measurements of the B hadron lifetimes are important to test our understanding of B hadron decay dynamics. In the naive spectator model, one expects $\tau(B^+) = \tau(B_s^0) = \tau(B_d^0) = \tau(\Lambda_b)$. However, a strong hierarchy is observed in the case of charm hadrons: $\tau(D^+) \simeq 2.3\ \tau(D_s) \simeq 2.5\ \tau(D^0) \simeq 5\ \tau(\Lambda_c^+)$. This hierarchy is predicted to scale with $1/m_Q^2$ and is thus expected to yield much smaller lifetime differences for B hadrons. A calculation [2], based on an expansion in terms of $1/m_Q$, predicts the lifetimes for different B hadrons to be less than 10%.

Several techniques have been used to measure the B^+ and B_d^0 lifetimes. The cleanest method reconstructs samples of B^+ and B_d^0 decays exclusively but suffers from small branching fractions ($\sim 10^{-4} - 10^{-3}$). Most measurements have relied on samples of semileptonic B decays where the $D^{(*)}$ meson is exclusively reconstructed and intersected with an identified lepton to determine the B decay point. The two techniques used by SLD take advantage of the excellent 3-D vertexing capabilities of the CCD Vertex Detector to reconstruct the decays (semi-) inclusively. The goal is to reconstruct and identify all the tracks originating from the B decay chain, and thus separate charged and neutral B mesons using the total charge Q of tracks associated with the decay.

The first analysis [3] uses an inclusive topological vertexing technique [4] summarized below. A search is made to find regions in 3-D space with high track density (other than the primary vertex). Such a region, or "seed" vertex, is found in $\sim 50\%$ of b hemispheres, but only in $\sim 15\%$ of c hemispheres and in less than 1% of uds hemispheres. The b hemisphere vertex finding efficiency increases with the decay length D to attain a constant level of 80% for $D > 3$ mm. Due to the typical $B \rightarrow D$ cascade structure of the decays, not all tracks originate from a single space point, and thus, may not be attached to the seed vertex if the D meson travelled sufficiently far from the B decay point. Therefore, isolated tracks with $T < 1$ mm and $L/D > 0.3$ are attached to the seed vertex to form the final secondary vertex. The quantity T represents the minimum distance between a given track and the seed vertex axis, and L is the distance along the vertex axis between the interaction point and the point of closest approach between the track and the vertex axis.

In the hadronic Z^0 event sample, we select 9719 B decay candidates by requiring the decay length $D > 1$ mm and the invariant mass computed using all tracks associated with the secondary vertex $M_{raw} > 2$ GeV/c^2. The minimum vertex mass requirement serves not only as a means to select a 97% pure sample of $b\bar{b}$ events but also as a means to enhance the charge reconstruction purity. The sample is divided into 3665 neutral and 6033 charged decays with $Q = 0$ and $Q = \pm 1, 2, 3$, respectively. Monte Carlo (MC) studies show that the charged sample consists of 52.8% B^+, 32.1% B_d^0, 8.6% B_s^0, and 4.3% B baryons, whereas the neutral sample consists of 25.3% B^+, 52.9% B_d^0, 13.9% B_s^0, and 6.2% B baryons[1]. The sensitivity of this analysis to the individual B^+ and B_d^0 lifetimes can be assessed from the 1.6 (2.1) ratio of B^+ (B_d^0) decays over B_d^0 (B^+) decays in the charged (neutral) sample.

The B^+ and B_d^0 lifetimes are extracted with a simultaneous binned maximum likelihood fit to the decay length distributions of the charged and neutral samples (Fig. 1). These distributions are compared with MC distributions obtained for a range of values of the B^+ and B_d^0 lifetimes. The maximum likelihood fit yields lifetimes of $\tau_{B+} = 1.67 \pm 0.07(\text{stat}) \pm 0.06(\text{syst})$ ps, $\tau_{B_d^0} = 1.66 \pm 0.08(\text{stat}) \pm 0.08(\text{syst})$ ps, with a ratio of $\tau_{B+}/\tau_{B_d^0} = 1.01^{+0.09}_{-0.08}(\text{stat}) \pm 0.05(\text{syst})$. The main contributions to the systematic error

---

[1] Reference to a specific state (e.g., B^+) implicitly includes its charge conjugate state (i.e., B^-).

Figure 1. Decay length distributions for data (points) and best fit MC (histogram) in the topological analysis.
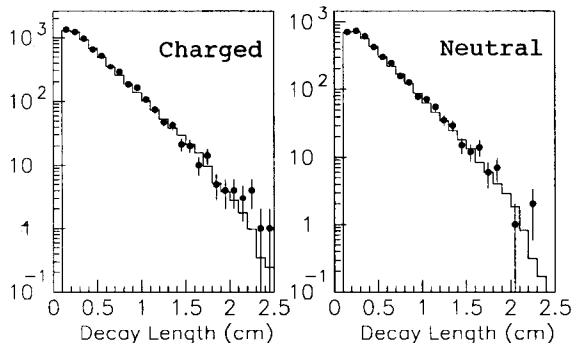

Figure 2. Decay length distributions for data (points) and best fit MC (histogram) in the semileptonic analysis.

come from uncertainties in the detector modeling, B_s^0 lifetime, fit systematics, and MC statistics.

The second lifetime analysis [3] is restricted to semileptonic decays. This reduces the overall efficiency compared to the topological method but results in an improved charge reconstruction purity. In this method, a D decay vertex is reconstructed topologically and the B decay vertex is formed by intersecting the D meson trajectory with that of an identified lepton. An attempt is then made to attach a slow-pion candidate to the B vertex to reconstruct the track topology of B decays into D^{*+} mesons.

The analysis selects identified electrons and muons with momentum transverse to the nearest jet axis > 0.4 GeV/c and results in a sample of 634 charged and 584 neutral decays. MC studies show that the remaining charged (neutral) sample is 97.4% (98.9%) pure in B hadrons. The simulated flavor contents are 66.6% B^+, 22.9% B_d^0, 5.5% B_s^0, and 2.4% B baryons for the charged sample, and 19.5% B^+, 60.2% B_d^0, 14.8% B_s^0, and 4.4% B baryons for the neutral sample. The sensitivity of this analysis to the individual B^+ and B_d^0 lifetimes can be assessed from the 3:1 ratio of B^+ (B_d^0) decays over B_d^0 (B^+) decays in the charged (neutral) sample.

As for the topological analysis, the B^+ and B_d^0 lifetimes are extracted from the decay length distributions of the charged and neutral samples (Fig. 2). The fit yields:
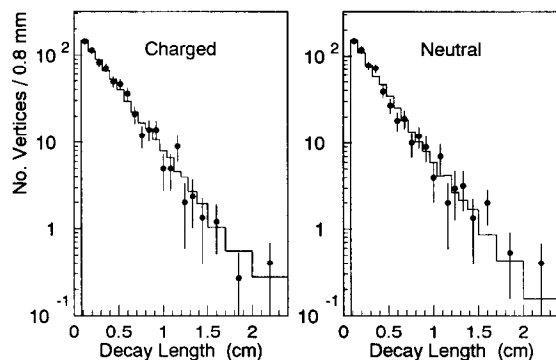
$\tau_{B+} = 1.61^{+0.13}_{-0.12}(\text{stat}) \pm 0.07(\text{syst})$ ps, $\tau_{B_d^0} = 1.56^{+0.14}_{-0.13}(\text{stat}) \pm 0.10(\text{syst})$ ps, with a ratio of $\tau_{B+}/\tau_{B_d^0} = 1.03^{+0.16}_{-0.14}(\text{stat}) \pm 0.09(\text{syst})$. The dominant sources of systematic error are the same as for the topological analysis.

The two analyses described above yield lifetime measurements in agreement with those from other experiments and with the expectation that the B^+ and B_d^0 lifetimes are nearly equal.

3. B^0–$\overline{B^0}$ MIXING

Transitions between flavor states $B^0 \to \overline{B^0}$ take place via second order weak interactions "box diagrams." As in the case of the $K^0 - \overline{K^0}$ system, the weak eigenstates are linear combinations of the flavor eigenstates. Due to the difference in mass between the weak eigenstates, they propagate differently in time, which gives rise to time-dependent oscillations between B^0 and $\overline{B^0}$ flavor eigenstates. The oscillation frequency Δm_d for B_d^0–$\overline{B_d^0}$ mixing depends on the Cabibbo-Kobayashi-Maskawa (CKM) matrix element $|V_{td}|$ for which little is known experimentally. Theoretical uncertainties [5] are significantly reduced for the ratio between Δm_d and Δm_s. Thus, combining measurements of the oscillation frequency of both B_d^0–$\overline{B_d^0}$ and B_s^0–$\overline{B_s^0}$ mixing translates into a measurement of the ratio $|V_{td}|/|V_{ts}|$.

Experimentally, a measurement of the time dependence of B^0–$\overline{B^0}$ mixing requires three ingredients: (i) the B decay proper time has to be

3

reconstructed, (ii) the B flavor at production (initial state $t = 0$) needs to be determined, as well as (iii) the B flavor at decay (final state $t = t_{decay}$). At SLD, the time dependence of B_d^0-$\overline{B_d^0}$ mixing has been measured using four different methods. All four use the same initial state tagging but differ by the method used to either reconstruct the B decay or tag its final state.

Initial state tagging takes advantage of the large polarization-dependent forward backward asymmetry in $Z^0 \rightarrow b\bar{b}$ decays

$$\tilde{A}_{FB}(\cos\theta_T) = 2A_b \frac{A_e - P_e}{1 - A_e P_e} \frac{\cos\theta_T}{1 + \cos^2\theta_T}, \quad (1)$$

where $A_b = 0.94$ and $A_e = 0.15$. This only requires knowledge of the electron beam polarization P_e and the cosine of the angle between the thrust axis direction $\hat{T}$ and the electron beam direction, $\cos\theta_T$. For left- (right-) handed electrons and forward (backward) B decay vertices, the initial quark is tagged as a b quark; otherwise, it is tagged as a $\bar{b}$ quark. The initial state tag can be augmented by using a momentum-weighted track charge in the hemisphere opposite that of the reconstructed B vertex, defined as

$$Q_{jet} = \sum Q_i \left| \vec{p_i} \cdot \hat{T} \right|^\kappa \text{sign}\left(\vec{p_i} \cdot \hat{T}\right), \quad (2)$$

where $\vec{p_i}$ is the three-momentum of track i and Q_i its charge, and $\kappa = 0.5$. Figure 3 shows the distributions of $\cos\theta_T$ signed by the electron beam helicity and opposite hemisphere jet charge. Clear
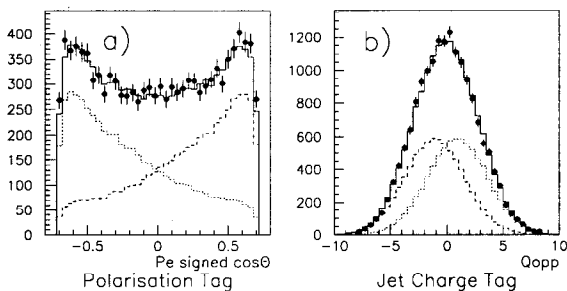

Figure 3. Distributions of (a) polarization-signed $\cos\theta_T$ and (b) opposite hemisphere jet charge for data (points) and MC (solid line). The MC b and $\bar{b}$ components are shown with dotted and dashed lines respectively.

separation between initial b and $\bar{b}$ quarks is observed. These two tags are combined to yield an initial state tag with 100% efficiency and effective average right-tag probability of 84% (for $\langle P_e \rangle = 77\%$).

The first two B_d^0-$\overline{B_d^0}$ mixing analyses [6] use topological vertexing to select the tracks from the B decay and measure its decay length. A sample of 16803 vertices is selected after requiring the mass of all tracks in the vertex, corrected for the amount of missing transverse momentum, $M > 2$ GeV/c^2 (no explicit cut is placed on the decay length). The first analysis uses charged kaons from the B decay chain to tag the final state. This tag relies on the fact that most B decays occur via the dominant $b \rightarrow c \rightarrow s$ transition. Thus, K^- (K^+) tags $\overline{B_d^0}$ (B_d^0) decays. The fraction of charged kaons produced with the right sign has been measured to be $(82 \pm 5)\%$ in B_d^0 decays [7]. Charged kaons are identified with the Cherenkov Ring Imaging Detector, using both liquid and gas radiators to cover most of the kaon momentum range: 0.8 to 25 GeV/c. The rate of pion misidentification as a function of momentum is calibrated from the data using a pure sample of pions from K_s^0 decays. The kaon tag yields a sample of 5694 decays with a correct tag probability of 77% for B_d^0 decays.

The time dependence of B_d^0-$\overline{B_d^0}$ mixing is measured from the fraction of decays tagged as mixed as a function of decay length. A decay is tagged as mixed if the initial and final state tags disagree. A binned χ^2 fit is performed by comparing the distributions of the mixed fraction as a function of decay length obtained for the data and the MC for a range of Δm_d values. Figure 4(a) shows the mixed fraction distribution for the charged kaon analysis. The fit yields a frequency of $\Delta m_d = 0.580 \pm 0.066(\text{stat}) \pm 0.075(\text{syst})$ ps^{-1} with a $\chi^2/\text{dof} = 10.2/10$. The main contributions to the systematic error arise from uncertainties in the $\pi \rightarrow K$ misidentification calibration from the data, in the rate of right-sign kaon production in B^+ and B_d^0 decays, and in the dependence of the fit results on binning and fit range, as summarized in Table 1.

The second analysis exploits the $B \rightarrow D$ cascade charge structure to tag the final state. To enhance the B_d^0 fraction, we require the vertex

Table 1
Systematic uncertainties for the different Δm_d measurements (in ps^{-1}).

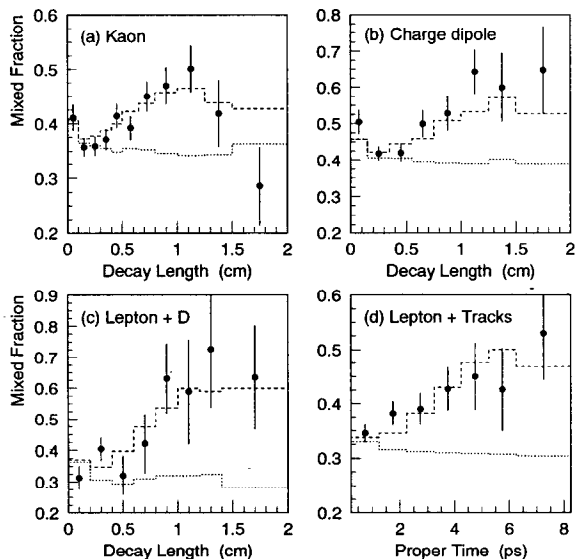| Analysis	Kaon	Charge Dipole	Lepton+D	Lepton+Tracks
Detector simulation	0.036	0.010	0.020	0.013
Physics modeling	0.048	0.027	0.024	0.032
Fit systematics	0.045	0.026	0.038	–
Total	0.075	0.039	0.049	0.035

Figure 4. Distributions of the fraction of decays tagged as mixed as a function of decay length or proper time for data (points) and best fit MC (dashed histograms) for the various analyses: (a) charged kaon, (b) charge dipole, (c) lepton + D, and (d) lepton + tracks. The dotted histograms correspond to MC distributions with no B_d^0–$\overline{B_d^0}$ mixing.

charge $Q = 0$. This requirement also improves the probability of correctly assigning all of the B_d^0 decay tracks. The direction of the vertex axis is adjusted to minimize the impact parameter sum of the tracks in the vertex and the mean track impact parameter is required to be less than 50 μm at this minimum. A sample of 3291 decays satisfies the selection criteria. The "charge dipole" δq of the vertex is then defined as the relative displacement between the weighted mean location

L_i of the positive tracks and of the negative tracks: $\delta q = (\sum^+ w_i L_i)/(\sum^+ w_i) - (\sum^- w_i L_i)/(\sum^- w_i)$, where the first (second) term is a sum over all positive (negative) tracks in the vertex. The weight w_i for each track i is inversely proportional to the uncertainty on the quantity L_i. The correct tag probability increases with the magnitude of δq and reaches a maximum of 84% at large $|\delta q|$. A fit to the mixed fraction distribution as a function of decay length [Fig. 4(b)] yields $\Delta m_d = 0.561 \pm 0.078(\text{stat}) \pm 0.039(\text{syst})$ ps^{-1} with a $\chi^2/\text{dof} = 8.8/7$. The main contributions to the systematic error come from MC statistics and fit systematics (Table 1).

The next two analyses select semileptonic decays. The first of these (lepton + D, Ref. [8]) is identical to that used to measure the B^+ and B_d^0 lifetimes. As for the charge dipole analysis, a set of neutral vertices is selected. The charge of the lepton tags the $B_d^0/\overline{B_d^0}$ flavor at decay with a correct tag probability of 85%. As for the above two analyses, a fit to the mixed fraction distribution [Fig. 4(c)] yields $\Delta m_d = 0.452 \pm 0.074(\text{stat}) \pm 0.049(\text{syst})$ ps^{-1} with a $\chi^2/\text{dof} = 7.8/7$. The systematic error is dominated by MC statistics and fit systematics (Table 1).

The last analysis (lepton+tracks, Ref. [9]) selects semileptonic decays by identifying electrons and muons with high transverse momentum $p_T > 0.8$ GeV/c with respect to the nearest jet axis. This enhances the fraction of $Z^0 \rightarrow b\bar{b}$ events and allows for the use of a fully inclusive vertexing technique. The B decay vertex is estimated by computing an average intersection point between the lepton trajectory and all well-measured tracks in the jet, each track being weighted according to its probability to originate from the decay of a short-lived heavy hadron. Here, the B decay proper time is reconstructed by estimating the B hadron momentum based on track and energy

clusters in the calorimeter. The final sample contains 2609 semileptonic decay candidates with an estimated B hadron purity of 93% and correct final state tag probability of 85%.

For this analysis, the value of Δm_d is extracted from an unbinned maximum likelihood analysis with parameterizations estimated from the MC. The fit yields $\Delta m_d = 0.520 \pm 0.072(\text{stat}) \pm 0.035(\text{syst})$ ps^{-1} and the corresponding mixed fraction distribution is shown in Fig. 4(d). Main systematic uncertainties are presented in Table 1.

The preliminary results from the four analyses have been combined, taking into account statistical and systematic correlations, to produce the following SLD average:

$$\Delta m_d = 0.525 \pm 0.043(\text{stat}) \pm 0.037(\text{syst}) \text{ ps}^{-1}. \quad (3)$$

This average is consistent with the world average value of 0.466 ± 0.018 [5].

4. SUMMARY AND FUTURE

Using a sample of $\sim 150,000$ hadronic Z^0 decays collected between 1993 and 1995, the SLD Collaboration has produced precise B^+ and B_d^0 lifetime measurements, as well as measurements of the time dependence of B_d^0–$\overline{B}_d^0$ mixing. In 1996, SLD installed an improved CCD Vertex Detector. This new detector allows for significant improvements in resolution. In particular, the decay length resolution improves by roughly a factor of two. SLD is looking forward to performing many exciting B physics measurements over the next few years.

REFERENCES

1. K. Abe et al., Phys. Rev. D **53**, 1023 (1996).
2. I. I. Bigi et al., in B Decays, ed. S. Stone (World Scientific, New York, 1994), p. 132.
3. K. Abe et al., to appear in Phys. Rev. Lett. **79** (1997).
4. D. Jackson, Nucl. Instrum. Methods A **388**, 247 (1997).
5. L. K. Gibbons, Status of Weak Quark Mixing, UR-1494, April 1997.
6. K. Abe et al., SLAC-PUB-7230, July 1996.
7. H. Albrecht et al., Z. Phys. C **62**, 371 (1994).
8. K. Abe et al., SLAC-PUB-7229, July 1996.
9. K. Abe et al., SLAC-PUB-7228, July 1996.

*K. Abe,[19] K. Abe,[30] T. Akagi,[28] N.J. Allen,[4] W.W. Ash,[28]† D. Aston,[28] K.G. Baird,[16] C. Baltay,[34] H.R. Band,[33] M.B. Barakat,[34] G. Baranko,[9] O. Bardon,[15] T. L. Barklow,[28] G.L. Bashindzhagyan,[18] A.O. Bazarko,[10] R. Ben-David,[34] A.C. Benvenuti,[2] G.M. Bilei,[22] D. Bisello,[21] G. Blaylock,[16] J.R. Bogart,[28] B. Bolen,[17] T. Bolton,[10] G.R. Bower,[28] J.E. Brau,[20] M. Breidenbach,[28] W.M. Bugg,[29] D. Burke,[28] T.H. Burnett,[32] P.N. Burrows,[15] W. Busza,[15] A. Calcaterra,[12] D.O. Caldwell,[5] D. Calloway,[28] B. Camanzi,[11] M. Carpinelli,[23] R. Cassell,[28] R. Castaldi,[23](a) A. Castro,[21] M. Cavalli-Sforza,[6] A. Chou,[28] E. Church,[32] H.O. Cohn,[29] J.A. Coller,[3] V. Cook,[32] R. Cotton,[4] R.F. Cowan,[15] D.G. Coyne,[6] G. Crawford,[28] A. D'Oliveira,[7] C.J.S. Damerell,[25] M. Daoudi,[28] R. De Sangro,[12] R. Dell'Orso,[23] P.J. Dervan,[4] M. Dima,[8] D.N. Dong,[15] P.Y.C. Du,[29] R. Dubois,[28] B.I. Eisenstein,[13] R. Elia,[28] E. Etzion,[33] S. Fahey,[9] D. Falciai,[22] C. Fan,[9] J.P. Fernandez,[6] M.J. Fero,[15] R. Frey,[20] K. Furuno,[20] T. Gillman,[25] G. Gladding,[13] S. Gonzalez,[15] E.L. Hart,[29] J.L. Harton,[8] A. Hasan,[4] Y. Hasegawa,[30] K. Hasuko,[30] S. J. Hedges,[3] S.S. Hertzbach,[16] M.D. Hildreth,[28] J. Huber,[20] M.E. Huffer,[28] E.W. Hughes,[28] H. Hwang,[20] Y. Iwasaki,[30] D.J. Jackson,[25] P. Jacques,[24] J. A. Jaros,[28] A.S. Johnson,[3] J.R. Johnson,[33] R.A. Johnson,[7] T. Junk,[28] R. Kajikawa,[19] M. Kalelkar,[24] H. J. Kang,[26] I. Karliner,[13] H. Kawahara,[28] H.W. Kendall,[15] Y. D. Kim,[26] M.E. King,[28] R. King,[28] R.R. Kofler,[16] N.M. Krishna,[9] R.S. Kroeger,[17] J.F. Labs,[28] M. Langston,[20] A. Lath,[15] J.A. Lauber,[9] D.W.G.S. Leith,[28] V. Lia,[15] M.X. Liu,[34] X. Liu,[6] M. Loreti,[21] A. Lu,[5] H.L. Lynch,[28] J. Ma,[32] G. Mancinelli,[22] S. Manly,[34] G. Mantovani,[22] T.W. Markiewicz,[28] T. Maruyama,[28] H. Masuda,[28] E. Mazzucato,[11] A.K. McKemey,[4] B.T. Meadows,[7] R. Messner,[28] P.M. Mockett,[32] K.C. Moffeit,[28] T.B. Moore,[34] D. Muller,[28] T. Nagamine,[28] S. Narita,[30] U. Nauenberg,[9] H. Neal,[28] M. Nussbaum,[7] Y. Ohnishi,[19] L.S. Osborne,[15] R.S. Panvini,[31] C.H. Park,[27] H. Park,[20] T.J. Pavel,[28] I. Peruzzi,[12](b) M. Piccolo,[12] L. Piemontese,[11] E. Pieroni,[23] K.T. Pitts,[20] R.J. Plano,[24] R. Prepost,[33] C.Y. Prescott,[28] G.D. Punkar,[28] J. Quigley,[15] B.N. Ratcliff,[28] T.W. Reeves,[31] J. Reidy,[17] P.L. Reinertsen,[6] P.E. Rensing,[28] L.S. Rochester,[28] P.C. Rowson,[10] J.J. Russell,[28] O.H. Saxton,[28] T. Schalk,[6] R.H. Schindler,[28] B.A. Schumm,[6] S. Sen,[34] V.V. Serbo,[33] M.H. Shaevitz,[10] J.T. Shank,[3] G. Shapiro,[14] D.J. Sherden,[28] K.D. Shmakov,[29] C. Simopoulos,[28] N.B. Sinev,[20] S.R. Smith,[28] M.B. Smy,[8] J.A. Snyder,[34] P. Stamer,[24] H. Steiner,[14] R. Steiner,[1] M.G. Strauss,[16] D. Su,[28] F. Suekane,[30] A. Sugiyama,[19] S. Suzuki,[19] M. Swartz,[28] A. Szumilo,[32] T. Takahashi,[28] F.E. Taylor,[15] E. Torrence,[15] A.I. Trandafir,[16]

J.D. Turk,[34] T. Usher,[28] J. Va'vra,[28]
C. Vannini,[23] E. Vella,[28] J.P. Venuti,[31]
R. Verdier,[15] P.G. Verdini,[23] D.L. Wagner,[9]
S.R. Wagner,[28] A.P. Waite,[28] S.J. Watts,[4]
A.W. Weidemann,[29] E.R. Weiss,[32] J.S. Whitaker,[3]
S.L. White,[29] F.J. Wickens,[25] D.A. Williams,[6]
D.C. Williams,[15] S.H. Williams,[28] S. Willocq,[28]
R.J. Wilson,[8] W.J. Wisniewski,[28] M. Woods,[28]
G.B. Word,[24] J. Wyss,[21] R.K. Yamamoto,[15]
J.M. Yamartino,[15] X. Yang,[20] J. Yashima,[30]
S.J. Yellin,[5] C.C. Young,[28] H. Yuta,[30]
G. Zapalac,[33] R.W. Zdarko,[28] and J. Zhou,[20]

(The SLD Collaboration)

[1] *Adelphi University, Garden City, New York 11530*
[2] *INFN Sezione di Bologna, I-40126 Bologna, Italy*
[3] *Boston University, Boston, Massachusetts 02215*
[4] *Brunel University, Uxbridge, Middlesex UB8 3PH,
United Kingdom*
[5] *University of California at Santa Barbara, Santa
Barbara, California 93106*
[6] *University of California at Santa Cruz, Santa Cruz,
California 95064*
[7] *University of Cincinnati, Cincinnati, Ohio 45221*
[8] *Colorado State University, Fort Collins, Colorado
80523*
[9] *University of Colorado, Boulder, Colorado 80309*
[10] *Columbia University, New York, New York 10027*
[11] *INFN Sezione di Ferrara and Università di Ferrara,
I-44100 Ferrara, Italy*
[12] *INFN Lab. Nazionali di Frascati, I-00044 Frascati,
Italy*
[13] *University of Illinois, Urbana, Illinois 61801*
[14] *Lawrence Berkeley Laboratory, University of
California, Berkeley, California 94720*
[15] *Massachusetts Institute of Technology, Cambridge,
Massachusetts 02139*
[16] *University of Massachusetts, Amherst,
Massachusetts 01003*
[17] *University of Mississippi, University, Mississippi
38677*
[18] *Moscow State University, Institute of Nuclear
Physics 119899 Moscow, Russia*
[19] *Nagoya University, Chikusa-ku, Nagoya 464 Japan*
[20] *University of Oregon, Eugene, Oregon 97403*
[21] *INFN Sezione di Padova and Università di Padova,
I-35100 Padova, Italy*
[22] *INFN Sezione di Perugia and Università di Perugia,
I-06100 Perugia, Italy*
[23] *INFN Sezione di Pisa and Università di Pisa,
I-56100 Pisa, Italy*
[24] *Rutgers University, Piscataway, New Jersey 08855*
[25] *Rutherford Appleton Laboratory, Chilton, Didcot,
Oxon OX11 0QX United Kingdom*
[26] *Sogang University, Seoul, Korea*
[27] *Soongsil University, Seoul, Korea 156-743*
[28] *Stanford Linear Accelerator Center, Stanford
University, Stanford, California 94309*
[29] *University of Tennessee, Knoxville, Tennessee 37996*
[30] *Tohoku University, Sendai 980 Japan*
[31] *Vanderbilt University, Nashville, Tennessee 37235*
[32] *University of Washington, Seattle, Washington
98195*
[33] *University of Wisconsin, Madison, Wisconsin 53706*
[34] *Yale University, New Haven, Connecticut 06511*
†*Deceased*
[a] *Also at the Università di Genova*
[b] *Also at the Università di Perugia*